Journal of Thrombosis and Haemostasis, **12**: 2120–2130 DOI: 10.1111/jth.12738

ORIGINAL ARTICLE

Stalled cerebral capillary blood flow in mouse models of essential thrombocythemia and polycythemia vera revealed by *in vivo* two-photon imaging

T. P. SANTISAKULTARM,*[1] C. Q. PADUANO,* T. STOKOL,† T. L. SOUTHARD,‡ N. NISHIMURA,* R. C. SKODA,§ W. L. OLBRICHT,*¶ A. I. SCHAFER,** R. T. SILVER** and C. B. SCHAFFER*

**Department of Biomedical Engineering, Cornell University; †Department of Population Medicine and Diagnostic Services, College of Veterinary Medicine, Cornell University; ‡Department of Biomedical Sciences, College of Veterinary Medicine, Cornell University, Ithaca, NY, USA; §Department of Biomedicine, University Hospital Basel, Basel, Switzerland; ¶Department Chemical and Biomolecular Engineering, Cornell University, Ithaca; and **Department of Medicine, Weill Cornell Medical College, New York, NY, USA*

To cite this article: Santisakultarm TP, Paduano CQ, Stokol T, Southard TL, Nishimura N, Skoda RC, Olbricht WL, Schafer AI, Silver RT, Schaffer CB. Stalled cerebral capillary blood flow in mouse models of essential thrombocythemia and polycythemia vera revealed by *in vivo* two-photon imaging. *J Thromb Haemost* 2014; **12**: 2120–30.

Summary. *Background:* Essential thrombocythemia (ET) and polycythemia vera (PV) are myeloproliferative neoplasms (MPNs) that share the $JAK2^{V617F}$ mutation in hematopoietic stem cells, leading to excessive production of predominantly platelets in ET, and predominantly red blood cells (RBCs) in PV. The major cause of morbidity and mortality in PV and ET is thrombosis, including cerebrovascular occlusive disease. *Objectives:* To identify the effect of excessive blood cells on cerebral microcirculation in ET and PV. *Methods:* We used two-photon excited fluorescence microscopy to examine cerebral blood flow in transgenic mouse models that mimic MPNs. *Results and conclusions:* We found that flow was 'stalled' in an elevated fraction of brain capillaries in ET (18%), PV (27%), mixed MPN (14%) and secondary (non-MPN) erythrocytosis (27%) mice, as compared with controls (3%). The fraction of capillaries with stalled flow increased when the hematocrit value exceeded 55% in PV mice, and the majority of stalled vessels contained only stationary RBCs. In contrast, the majority of stalls in ET mice were caused by platelet aggregates. Stalls had a median persistence time of 0.5 and 1 h in ET and PV mice, respectively. Our findings shed new light on potential mechanisms of neurological problems in patients with MPNs.

Keywords: animal models; cerebrovascular circulation; microcirculation; myeloproliferative disorders; optical imaging.

Correspondence: Chris B. Schaffer, B57 Weill Hall, Department of Biomedical Engineering, Cornell University, Ithaca, NY 14853, USA.
Tel.: +1 607 342 7737; fax: +1 607 255 7330.
E-mail: cs385@cornell.edu

[1]Present Address: National Institute of Neurological Disorders and Stroke, National Institutes of Health, Bethesda, MD, USA

Received 30 April 2014
Manuscript handled by: P. de Moerloose
Final decision: P. H. Reitsma, 28 August 2014

Introduction

Essential thrombocythemia (ET) and polycythemia vera (PV) are two of the chronic myeloproliferative neoplasms (MPNs), diseases characterized by hyperactivity of hematopoietic stem cells and their myeloid progenitors in the bone marrow [1]. Polycythemia vera is characterized primarily by an increased number of red blood cells (RBCs) that is often associated with an increase in circulating leukocytes and platelets; in contrast, essential thrombocythemia (ET) predominantly involves increased numbers of platelets, occasionally increased leukocytes but always a normal number of RBCs. The major causes of morbidity and mortality in both ET and PV are associated with clinical complications related to blood circulation and coagulation abnormalities [2]. However, the basic mechanisms of vascular occlusive complications in these disorders are poorly understood, largely because they have not been directly visualized and measured in real-time *in vivo* in the past. In PV, excess RBCs contribute to high blood viscosity that increases vascular resistance and slows blood flow [3]. Elevated leukocyte counts may also increase resistance in microvessels, where leukocytes must flow in single file. Further, elevated platelet counts and hyperactive platelets have been thought to lead to increased thrombosis in ET and PV, resulting in vessel occlusions. While these vascular problems are systemic and affect many organs, they can have devastating

consequences in the brain. In both ET and PV, occlusion of brain blood vessels is a frequent complication that leads to transient ischemic attacks and cerebral infarcts [4,5]. Obstructions in small brain vessels, which have not been observed directly, could also have a significant impact on neuronal health, even in the absence of acute symptoms. Clinical evidence shows that cerebral microinfarcts are associated with more precipitous cognitive decline and a higher risk of the development of dementia [6–8]. Some clinical case studies have identified cognitive problems in ET and PV patients in the absence of large vessel stroke [9–12]. Dysfunction in the microcirculation of the brain could play a role in such neurological symptoms.

The Janus kinase-signal transducers and activators of transcription (JAK-STAT) signaling pathway is critical for the control of hematopoiesis. A mutant form of one of the four cytoplasmic tyrosine kinases in this pathway, $JAK2^{V617F}$, has been found to be present in virtually all patients with PV and about 60% of those with ET [13–16]. Normally, STAT molecules are phosphorylated by activated JAK2 only after a cognate growth factor ligand, such as erythropoietin or thrombopoietin, binds to its cytokine receptor on hematopoietic cell surfaces. Phosphorylated STAT then translocates to the nucleus, promoting production of blood cells. With mutant $JAK2^{V617F}$, however, STAT phosphorylation is constitutively activated, irrespective of engagement of an extracellular signal, leading to excessive hematopoiesis [16]. Transgenic mice with this mutation were recently created. In these mice, a higher allele burden of $JAK2^{V617F}$ leads to a PV phenotype (increases in RBCs, and sometimes increases in leukocytes and/or platelets), whereas lower levels of the mutant gene lead to an ET phenotype (increases in platelets) [17]. These transgenic animals provide the opportunity to study brain blood flow disruptions in ET and PV.

To directly visualize and quantify the effects of MPN on brain blood flow, we examined vascular structure and cerebral blood flow in mouse models of these diseases using two-photon excited fluorescence (2PEF) microscopy, which enables three-dimensional imaging with micrometer resolution deep into brain tissue [18,19]. We examined wild-type, erythropoietin-injected (Epo-inj) and $JAK2^{V617F}$ transgenic mice with PV, ET or a mixed MPN phenotype. Using 2PEF microscopy, we quantified blood flow speed and vessel diameter in arterioles, capillaries and venules. Because we observed capillaries with spontaneously stalled blood flow in the MPN mice, we also quantified the fraction of capillaries with stalled blood flow and determined the types of cells lodged in stalled capillary segments.

Methods

Animal models

Six experimental groups of mice were used in this study: (i) wild-type (wt); (ii) bone marrow transplanted (BMT) wt; (iii) erythropoietin injected (Epo-inj) wt; (iv) $JAK2^{V617F}$ BMT mice with an ET phenotype (BMT ET); (v) $JAK2^{V617F}$ BMT mice with a PV phenotype (BMT PV); and (vi) $JAK2^{V617F}$ BMT mice with an MPN phenotype that did not fall into classical ET or PV diagnosis (BMT mixed MPN). All mice were on the C57/Bl6 background. BMT ET, BMT PV and BMT mixed MPN groups were chimeric mice, derived by bone marrow transplant from mutant $JAK2^{V617F}$ mice into wild-type mice [17]. For these groups, mice with spun hematocrit values above 54% were classified as PV; those with platelet counts above 3000 thou μL^{-1} without elevated hematocrit values were considered ET. Mice that did not exhibit these classical manifestations of ET and PV were included in the mixed MPN group. These animals showed laboratory evidence of MPNs (e.g. leukocytosis and bone marrow fibrosis [20]), but could not be unambiguously classified as ET or PV (patients with these phenotypically mixed or 'overlap' MPNs are likewise encountered in clinical practice). To control for the effects of the BMT procedure, we created an experimental group where lethally irradiated wt mice received normal bone marrow cells from another wt donor. The Epo-inj group of wt mice received 0.5 mL of erythropoietin (20–200 IU mL^{-1}) subcutaneously for five consecutive days to induce erythrocytosis, followed by an imaging experiment on day 8. This group served as a secondary polycythemia (secondary erythrocytosis), non-MPN model. For most mice we obtained the spun hematocrit value and for many we obtained the complete blood count and bone marrow histopathology. Characteristics of the mice in all six groups are summarized in Table 1. Because not all animals are used for all types of measurements, Table S1 shows the number of animals used for each measurement made in this paper.

In vivo *two-photon excited fluorescence imaging*

We followed previously published surgical procedures to gain optical access to the brain for acute imaging experiments [21] (Fig. 1A). The care and experimental manipulation of our animals have been reviewed and approved by the Institutional Animal Care and Use Committee at Cornell University. We imaged the cerebral vasculature of anesthetized mice using a custom-built 2PEF microscope [21] (Fig. 1B–D). Texas Red-dextran (0.05 mL of 2.5% w/v; D1830; Invitrogen, Carlsbad, CA, USA) and Rhodamine 6G (0.05 mL of 0.1% w/v) in saline were injected retroorbitally. The Texas Red-dextran labels the blood plasma, allowing imaging of vascular topology and quantification of blood flow by tracking the motion of non-labeled RBCs. The lipophilic Rhodamine 6G labels leukocytes and platelets with high efficiency [22]. In some animals, Hoechst 33342 (0.05 mL of 0.5% w/v; H1399; Invitrogen) was injected to label cell nuclei and aid in distinguishing leukocytes from platelets. The fluorescence emission was relayed through bandpass filters, 460/50,

Table 1 Characteristics of study animals

	wt	BMT wt	BMT mixed MPN	BMT ET	Epo-inj wt	BMT PV
Subjects (*n*)	23	7	17	11	19	16
Male/female	20/3	3/4	6/11	8/3	9/10	4/12
Age (months)	4.7 (0.4–6.6), 17	6.8 (4.1–7.6)	5.9 (4.2–8.1)	5.3 (4.0–12.6)	4.5 (0.8–19.7), 15	5.9 (4.1–7.1)
Weight (g)	26 (20–36)	29 (21–33)	26 (20–32)	25 (20–33)	24 (18–28), 17	22 (19–28)
Hematocrit value (%)*	48 (41–52), 8	41 (36–46), 6	42 (30–49), 15	46 (39–50)	61 (40–71), 13	63 (54–91)
Hemoglobin (g dL^{-1})	15.7 (14.3–17.1), 2	15.8 (14.1–17.2), 4	14.7 (10.5–20.0), 5	15.4 (11.6–18.7), 8	21.1 (19.7–21.5), 4	23.5 (12.9–30.7), 6
Red blood cells (mil μL^{-1})	10.4 (9.2–11.6), 2	10.8 (9.8–11.2), 4	9.9 (7.5–14.3), 5	11.0 (7.2–13.7), 8	14.4 (13.9–14.9), 4	14.9 (8.7–18.4), 6
Leukocytes (thou μL^{-1})	3.7 (3.1–4.3), 2	9.5 (5.0–12.3), 4	11.4 (1.8–18.4), 5	23.2 (12.3–78.6), 8	3.5 (1.5–9.6), 4	8.0 (4.0–35.0), 6
Platelets (thou μL^{-1})	991 (976–1007), 2	803 (283–882), 4	984 (94–8355), 5	5727 (3711–8019), 8	574 (154–850), 4	389 (109–1190), 6

Values are expressed as median (range), number of animals measured when less than total. *Packed cell volume by centrifugation.

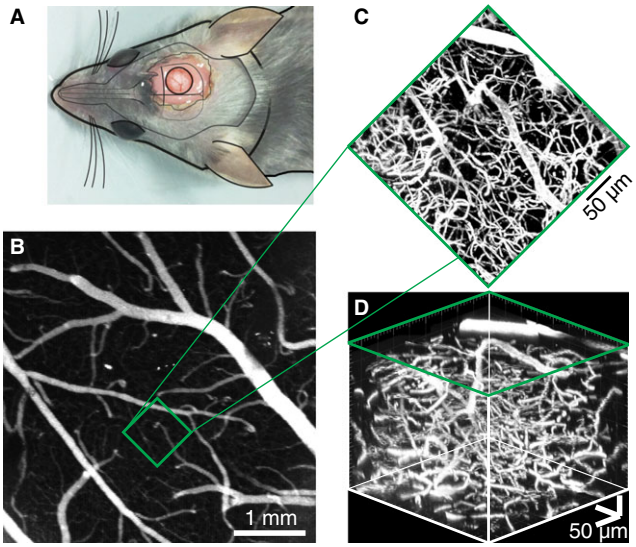

Fig. 1. *In vivo* 2PEF imaging of cortical microvessels. (A) Schematic drawing of a cranial window to allow optical access to the brain of an anesthetized mouse. (B) Low (4× air objective, NA = 0.28, Olympus) and (C) high (20× water immersion objective, NA = 0.95, Olympus) magnification 2PEF images of fluorescently-labeled brain vasculature. The images were obtained using a custom-built 2PEF microscope, and axially projected (z-direction) using ImageJ (National Institutes of Health). (D) Three-dimensional rendering (Imaris; Bitplane Scientific) of the vasculature beneath the brain surface.

575/25 and 645/65 nm (center wavelength/bandwidth), for Hoechst 33342, Rhodamine 6G and Texas Red-dextran, respectively. Laser scanning and data acquisition were controlled by MPSCOPE [23] or ScanImage [24]. RBC flow speed and vascular diameter of arteriole, venule and capillary vessel segments were measured using previously published methods [19,21,25].

Identifying stalled capillaries

Multiple overlapping 200 × 200 μm image stacks with 1-μm axial spacing up to 350 μm in cortical depth were recorded, and then aligned in three dimensions by maximizing the cross-correlation of fluorescence signal in the overlapping regions. Each vessel segment in the combined image stack was manually scored to be flowing or stalled based on the observed motion of RBCs, with the individual conducting this analysis blinded to the phenotype of the animal. Each capillary segment was visible for a minimum of 1 s in the image stack and we could easily detect cell motion of 1 μm over this time, so vessels classified as stalled had a maximum RBC speed of 1 μm s^{-1}, or about 1000 times slower than average cortical capillary flow speeds in mice [21]. Most stalled vessels clearly exhibited no discernable motion over the observation period. Our definition of a stalled capillary is based solely on motion of blood cells because motion of plasma could not be determined with our labeling scheme.

Platelets and leukocytes, both labeled by Rhodamine 6G, could be distinguished based on their appearance. Leukocytes were larger and showed solid fluorescence throughout the cell. Platelets were much smaller, tended to aggregate along vessel walls, and presented a more punctate appearance. We confirmed the identification of leukocytes based on colocalization of Hoechst 33342 and Rhodamine 6G in some animals. We further classified capillary stalls based on the cells present in the capillary. In some cases, platelets or leukocytes were present in stalled segments. In other cases, the stalled segment contained only stationary RBCs. Some stalled segments were designated as empty because they contained no cells, either stalled or flowing. To quantify stall persistence, we monitored the stability of capillary stalls in some animals by repeated imaging at 15, 30, 60 and 120 min. We determined whether or not stalled vessels reestablished flow over that time. However, it is possible that these stalled capillaries may have established flow, then stalled again between our observations. We also tracked the total number of capillary segments within the brain volumes we imaged in order to quantify vascular density.

Results

Blood flow was stalled in a large fraction of cortical capillaries in mouse models of PV, ET, mixed MPN and secondary erythrocytosis

In all animal groups, we found all surface and penetrating arterioles and all surface and ascending venules to be flowing. In wild-type animals, we found that the vast majority of brain capillaries were also flowing, with only a small fraction stalled: 3 ± 1% in wt (mean ± standard error of the mean (SEM); 3653 vessels, 14 mice) and 3 ± 1% in BMT wt (2325 vessels, three mice, no significant difference; Kruskal-Wallis with Dunn's multiple comparisons with wt group). In contrast, we found an increased fraction of capillaries with stalled blood flow in mice with MPN-specific mutant JAK2 in hematopoietic cells that exhibited an ET phenotype (18 ± 7%; 2815 vessels, five mice, $P = 0.1$), a mixed MPN phenotype (14 ± 3%; 8827 vessels, 15 mice, $P = 0.03$) or a PV phenotype (27 ± 4%; 8959 vessels, 13 mice, $P = 0.0001$; Fig. 2B). In addition, a significant elevation in the fraction of capillaries with stalled flow was found in the Epo-injection model of erythrocytosis (19 ± 4%; 5849 vessels, 15 mice, $P = 0.002$).

The fraction of capillaries with stalled flow in both models with excessive erythrocytosis, whether due to mutant JAK2 (causing PV) or erythropoietin injection (causing secondary polycythemia), increased abruptly, but with significant variability, when hematocrit values exceeded 55% (Fig. 2C). In the BMT ET and BMT mixed MPN animals, the fraction of capillaries with stalled flow did not show a dependence on hematocrit value (Fig. 2C). No animal groups showed a clear

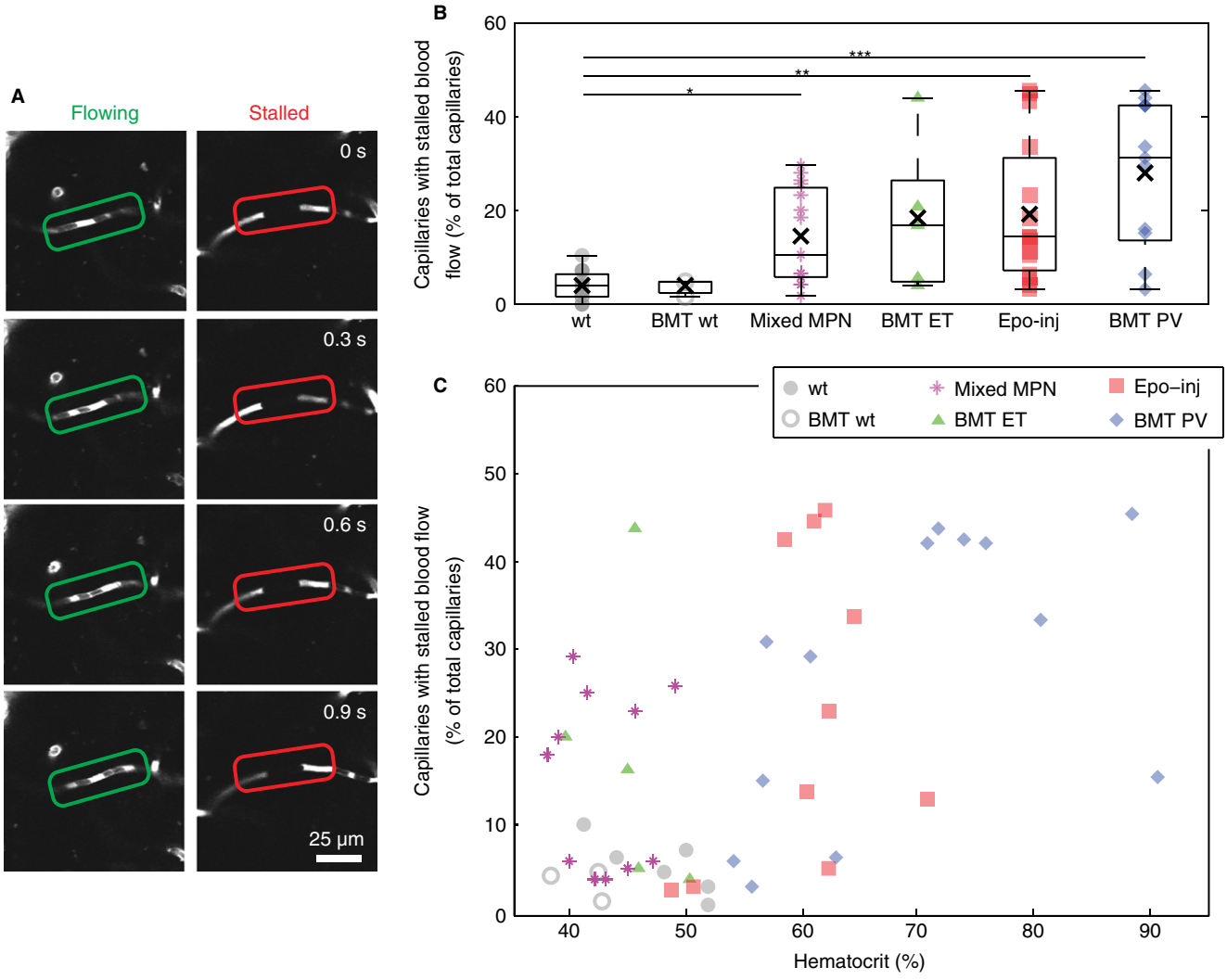

Fig. 2. Elevated capillary stalls in mouse models of ET, PV, mixed MPN and secondary erythrocytosis. (A) Sequential 2PEF images that demonstrate flowing (left panels) and stalled (right panels) capillaries in the cerebral cortex (images captured every 0.3 s for a total of 1.2 s of observation). Texas Red-dextran was intravenously injected to label blood plasma (bright), leaving the cellular components unlabeled (dark). (B) Box plots of the fraction of capillaries with stalled blood flow in wt, BMT wt, BMT mixed MPN, BMT ET, Epo-inj and BMT PV animals. (C) Fraction of capillaries with stalled blood flow as a function of hematocrit value for all animal groups. *$P = 0.03$; **$P = 0.002$; ***$P = 0.0001$.

dependence of the fraction of capillaries with stalled flow on leukocyte (Figure S1A) or platelet counts (Figure S1B), although these data were more limited.

RBCs and platelet aggregates contributed to microvascular stalls in PV and ET

To identify the cellular basis for these stalled capillaries, we developed a strategy to distinguish between several potential causes: (i) stationary RBCs (unlabeled objects with no other cell types present); (ii) platelet aggregates (punctate, clumped objects labeled by Rhodamine 6G); (iii) leukocyte plugs (cell-shaped objects labeled by Rhodamine 6G); or (iv) empty vessels (filled with blood plasma but no blood cells) (Fig. 3A, Video S1). All groups had statistically distinct distributions of causes of capillary stalls ($P < 0.001$, chi-square test). In the BMT ET group, platelet aggregates dominated and were responsible for 50% of all stalls, while stalls with only stationary RBCs were associated with 65%, 50% and 48% of the stalls in Epo-inj, BMT PV mice and BMT mixed MPN groups, respectively (Fig. 3B). Interestingly, the distribution of causes of capillary stalls was also significantly different between BMT PV mice and Epo-injected animals, with leukocyte plugs and platelet aggregates playing a larger role in the BMT PV mice ($P \leq 0.0004$).

Capillary stalls were persistent

In some animals, we monitored each stalled capillary with a leukocyte plug, platelet aggregates, stationary RBCs or empty of cells over about 2 h and performed a 'survival analysis' on stalled microvessels. Flow was reestablished most quickly in the BMT ET group (median stall persistence time of 30 min; 208 stalls, three mice), followed by the Epo-inj group (64 min; 999 stalls, eight mice), the BMT PV group (105 min; 856 stalls, 10 mice) and the BMT mixed MPN group (138 min; 430 stalls, 11 mice) (Fig. 3C). In the BMT ET group, nearly half of the stalls caused by platelet aggregates reestablished blood flow within the first 10 min (Figure S2B), which is reflected in the overall shorter stall persistence time (Fig. 3C). After approximately 2 h, $14 \pm 3\%$, $28 \pm 2\%$, $23 \pm 2\%$ and $79 \pm 1\%$ (mean $\pm$ SEM) of stalled capillaries in BMT ET, Epo-inj, BMT PV and BMT mixed MPN groups remained stalled, respectively. In some cases, we observed a capillary stall breaking and flow being reestablished. Figure 4 shows an example from a PV mouse, where three RBCs were stationary over the first 1.5 s of imaging, then abruptly began to flow at about 20 μm s^{-1}.

Quantification of average RBC flow speed, vessel diameter and capillary density

In arterioles, venules and capillaries that remained flowing, neither flow speed (Fig. 5A) nor vessel diameter

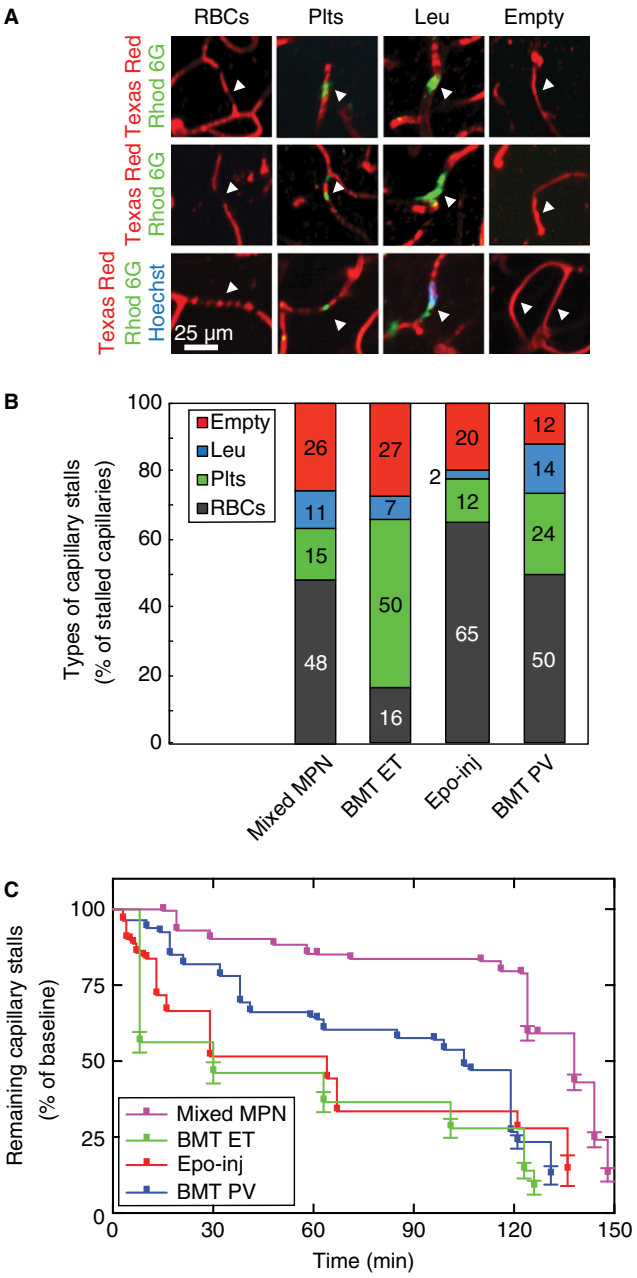

Fig. 3. Classes and persistence of microvascular stalls in ET, PV, mixed MPN and secondary erythrocytosis mouse models. (A) Four classes of microvascular stalls are distinguished: (i) stationary RBCs; (ii) platelet aggregates; (iii) leukocyte plugs; or (iv) empty plasma-filled vessels with no blood cells. Texas Red-dextran labeled blood plasma (red), Rhodamine 6G labeled leukocytes and platelets (green). Leukocyte plugs and platelet aggregates had distinct morphologies that could be differentiated from one another. To verify this, Hoechst 33342 dye was used to label nuclei of leukocytes (blue) in some animals. RBCs were unlabeled and appeared dark against the labeled blood plasma in each vessel. See also Video 1. (B) Classification of the cause of capillary stalls as a fraction of the total number of stalled capillaries for each mouse model. (C) Survival plot of capillary stalls that remain in place as function of time for each mouse model.

(Fig. 5B) was remarkably different between groups (Fig. 5C). The BMT PV mice, however, had nine of the 11 capillaries with flow speed below 200 μm s^{-1} as well

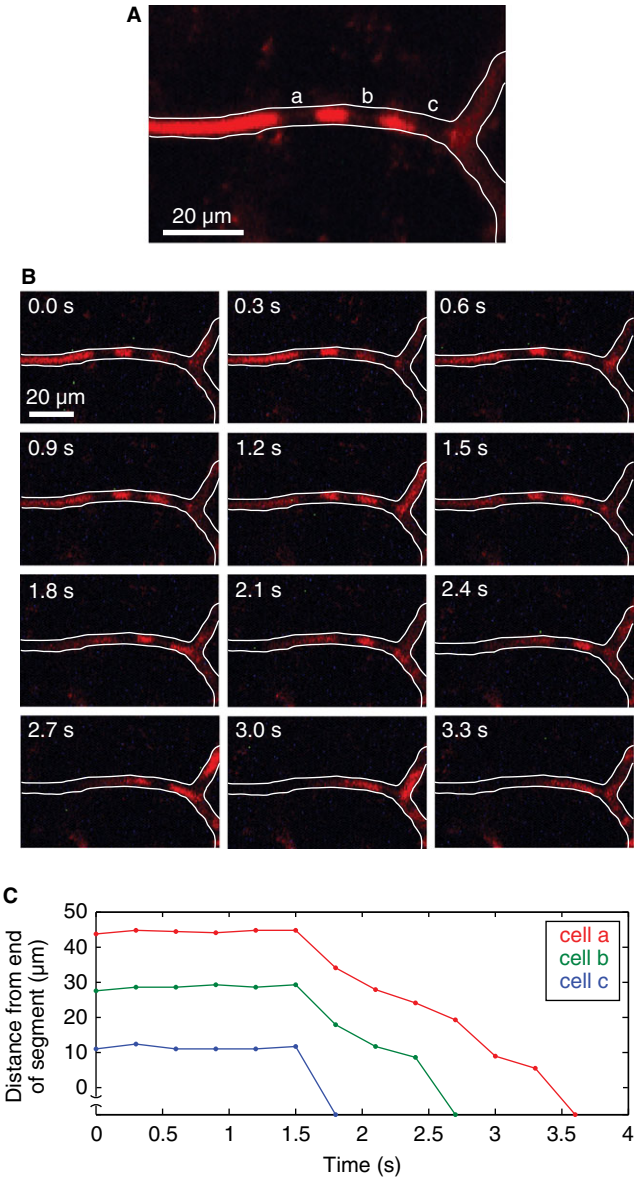

Fig. 4. Example of initially stationary RBCs breaking free, leading to reestablished blood flow, in a PV mouse. (A) High magnification, z-projected 2PEF image of a stalled cortical capillary. Texas Red-dextran, Rhodamine 6G and Hoechst 33342 were all used as labels, so the three dark objects within the vascular lumen were stationary RBCs (labeled *a*, *b* and *c*). (B) Sequential 2PEF images (every 0.3 s) showing stalled flow in the capillary segment until after 1.5 s of observation, when it began to flow. (C) Plot of the position of RBCs *a*, *b* and *c* relative to the end of the vascular segment over time. Once the capillary began to flow, the flow speed was about 20 μm s^{-1}.

as the four slowest arterioles that were measured across all animal groups, suggesting reduced flow even in vessels that were not stalled in BMT PV mice. Lastly, we manually counted the number of capillary segments in the imaged volume to estimate vascular density. We observed a large variability among animals within each group but no significant difference between groups (Figure S3).

Discussion

We studied cortical blood flow in mouse models of PV, ET, mixed MPN and secondary erythrocytosis and found a dramatic increase in the fraction of capillaries with stalled blood flow, as compared with control mice. As a control, we compared the results of wt and BMT wt animals and did not find gamma irradiation and bone marrow transplantation to have an impact on the outcome. While large vessel thrombosis does occur in humans with PV and ET (e.g. deep vein thrombosis [26], myocardial infarction and stroke [27]), we did not observe flow blockages in brain surface arterioles or venules that were larger than approximately 7-μm diameter. Consistent with our finding of stalled capillary flow in MPN mouse models, microvascular flow problems are frequently observed in humans. For example, a study of 103 $JAK2^{V617F}$-positive MPN patients reported that 12 had arterial thrombosis, seven had venous thrombosis and 11 had microvascular thrombosis, the latter accounting for half of all thrombotic complications that occurred prior to diagnosis with MPN [28]. Amongst 140 consecutive MPN patients, 22/80 with ET and 20/60 with PV had microcirculatory symptoms, a higher incidence than large vessel arterial and/or venous thrombosis [29].

Hematocrit value was found to be a strong predictor of the fraction of capillary segments with stalled flow in the BMT PV and Epo-inj animal groups in our study, but with significant variability in the fraction of capillaries with stalled flow at any given hematocrit. This finding may provide a scientific basis for the recently published findings of a clinical trial in PV patients showing that phlebotomy and/or hydroxyurea treatment targeted to reduce the hematocrit value to < 45% was associated with significantly lower rates of cardiovascular death and major thrombosis, as compared with patients treated for a higher hematocrit target value of 45–50% [30].

Our observation that RBC stalls in PV animals typically resolved by an abrupt clearance of the stationary RBCs, within 0.3 s or one image frame, followed by rapid RBC flow in the capillary segment, strongly suggests an adhesive mechanism. In recent work, RBCs from PV patients were found to have increased adhesion to endothelial cells as compared with controls [31,32]. Up-regulation and phosphorylation of the Lutheran/basal cell-adhesion molecule (Lu/BCAM) in circulating RBCs, which binds to endothelial cell laminin, was found to be the primary cause of this increased adhesion. The expression of Lu/BCAM in mature RBCs in wild-type mice has been found to be weak [33], although there have been few studies of the expression or activity of Lu/BCAM or other adhesion receptors on RBCs in murine disease models. In humans, $JAK2^{V617F}$ activity leads to up-regulation and phosphorylation of Lu/BCAM in RBCs [31,32], and this may also occur in mice. In a mouse model of hereditary spherocytosis, murine RBCs were

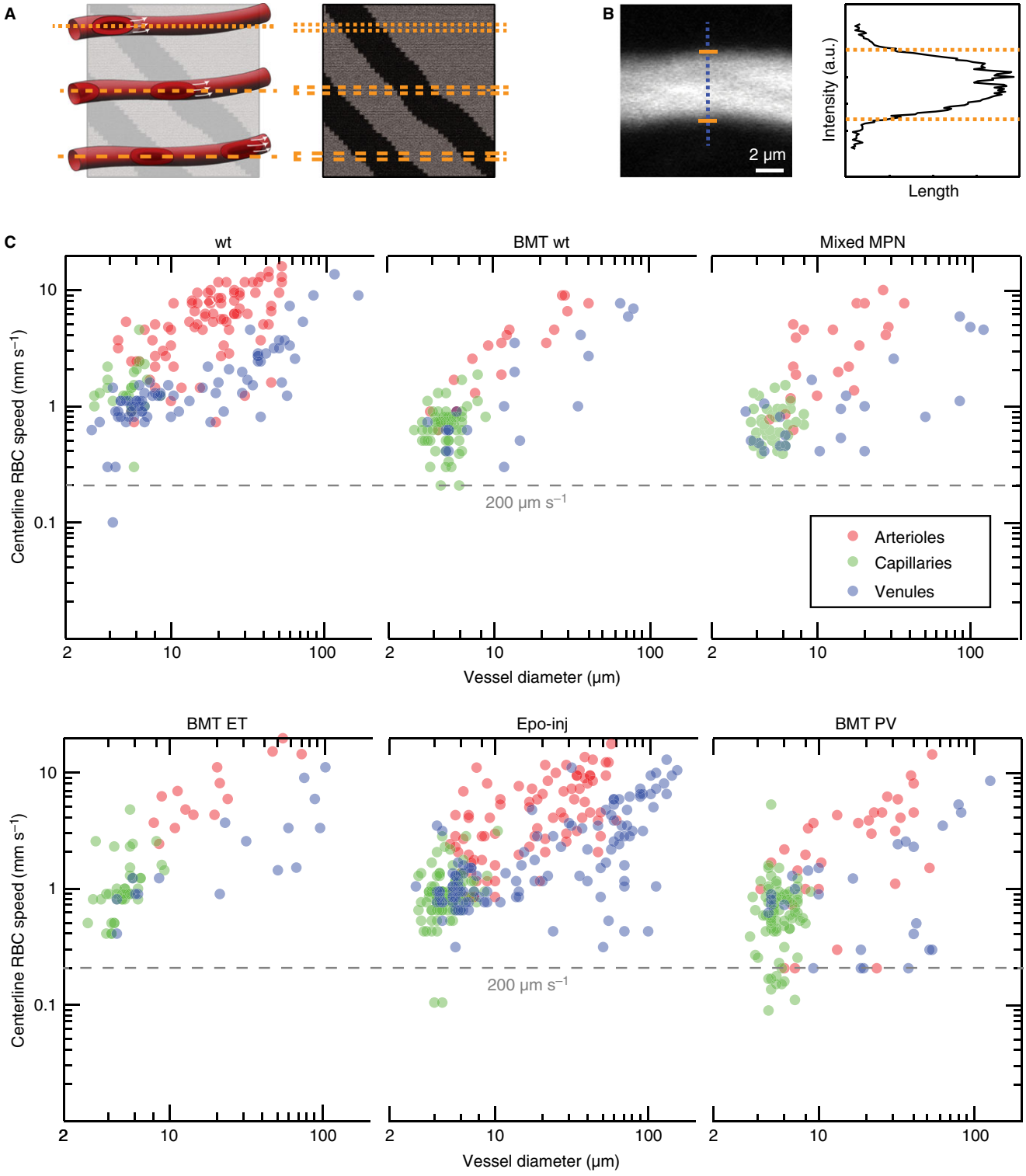

Fig. 5. Centerline RBC flow speed and vessel diameter in ET, PV, mixed MPN and secondary erythrocytosis mouse models. (A) Schematic drawing of linescan acquisition to track RBC positions over time and obtain centerline RBC flow velocity in individual blood vessels. (B) Axially projected (z-direction) image of a single microvessel and its intensity profile along the drawn line to determine vessel diameter. (C) Scatter plots of blood flow speed vs. vessel diameter for arterioles (red), capillaries (green) and venules (blue) for all animal groups.

observed to adhere to human laminin, suggesting that adhesion receptors can, indeed, be activated in murine RBCs in disease models [34].

Other factors may also play a role in the microcirculatory dysfunction we observed in our primary and secondary erythrocytosis models. High hematocrit values

increase blood viscosity, increasing vascular resistance and slowing flow. The cell-free layer that normally exists next to the vessel wall is also diminished due to margination of all blood cells. This phenomenon increases the likelihood and duration of interactions of cells with the endothelium, enhancing the probability of adhesion that could lead to a microvessel stall [35]. High hematocrit values, and hence, high viscosity, also generate abnormally high shear stress on the vessel wall that may facilitate endothelial dysfunction and activation of leukocytes and platelets [35–37]. In support of this, both leukocyte and platelet activation have been observed in patients with PV [38,39]. Together, such cellular activation would facilitate increased adhesion of leukocytes and platelets in the microvasculature [40]. Indeed, in the transgenic PV and Epo-injected animals, the compositions of stalled capillaries associated with RBCs, leukocytes, platelets and empty vessels were different. While the majority of stalled capillaries contained only stationary RBCs in both groups, leukocyte plugs and platelet aggregates were more common in the PV mice as compared with the Epo-injected animals, suggesting that leukocyte and platelet adhesion plays a larger role in the PV model as compared with the secondary erythrocytosis model.

The factors that influence the risk of vascular occlusion in ET remain unclear from previous studies. Hematocrit did not directly influence the fraction of capillaries with stalled flow, indicating a different mechanism for blood flow arrests as compared with PV. Although half of the stalled capillaries were caused by platelet aggregates in the ET group, neither platelet nor leukocyte counts were good predictors of the fraction of capillaries that were stalled in ET mouse models (or any of our mouse models). While platelet counts were elevated in all ET mice as compared with other groups, the fraction of capillaries stalled did not obviously increase with platelet number estimates (from blood smears) or with quantitative platelet counts (in the animals where they were available). The relationship between thrombocytosis, leukocytosis and vascular occlusive events in humans is similarly confounding. Both white count and platelet count have been found to be inconsistent predictors of the risk of large vessel thrombosis in MPN patients [37,41–43]. Leukocytosis was found to increase thrombotic risks in MPN patients in some studies [37,44,45]. On the other hand, one study found leukocytosis to have no impact on the incidence of thrombotic events [46]. In addition, although the World Health Organization does not include thrombocytosis as a risk factor for thrombotic events, its presence in ET patients is still considered to be a risk factor by some clinicians [43]. Therefore, further investigation is required to understand the roles of leukocytosis and thrombocytosis in microvascular disturbance.

We found the majority of capillary stalls in the $JAK2^{V617F}$ ET model to be caused by short-lived platelet aggregates, suggesting that platelet activation (rather than simple platelet numbers) may play a role in causing the stalls. In support of this idea, the percentage of platelets with high levels of P-selectin is increased in ET patients with a history of thrombosis compared with those without [47]. ET patients are also more likely to have an increase in soluble E-selectin, suggesting endothelial activation, and increased circulating microparticles, which amplify thrombogenesis [48,49]. Furthermore, prothrombin fragments, thrombomodulin and von Willebrand factor have been found to be elevated in both PV and ET [50], suggesting a prothrombotic environment. Leukocyte activation has also been observed and can result in an increase in circulating platelet-leukocyte complexes, which may also contribute to thrombosis [51,52]. Our results support the clinical observations that a prothrombotic flow environment is present in ET that could greatly affect the microcirculation. Our findings of fast flow reestablishment in stalls associated with platelet aggregates in ET mice may indicate somewhat weaker platelet adherence as compared with those found in macroscopic clots.

The notion that a primary endothelial cell defect may be a major cause of the microvascular stalls in the $JAK2^{V617F}$ bone marrow transplanted animals cannot be excluded by this study. It is certainly plausible because hematopoietic stem cell-derived endothelial progenitors may harbor the same abnormalities that occur in blood cells and might be, therefore, functionally abnormal as an antithrombotic surface [53].

Although the capillary stalls we have observed are not permanent, they persist for more than half an hour, on average, and thus may be analogous to very small strokes. In addition, having a large fraction of capillaries stalled, even when which vessels are stalled is constantly changing, causes chronic brain hypoperfusion that could further increase the prevalence of thrombotic [54] and neurological complications. Cortical microinfarcts and global hypoperfusion are recognized as common causes of cognitive decline and dementia in patients. The presence of silent brain infarcts alone, regardless of etiology, has been found to more than double the risk of developing dementia in a large-scale study involving over 1000 participants [6]. In addition to memory deficits, individuals with such small strokes showed a broad spectrum of cognitive and behavioral changes, including attentional and executive impairments as well as depression [7,8,55,56]. The microcirculatory problems we have observed in MPN mouse models could cause similar neurological dysfunction in PV and ET patients. In support of this, mouse models of excessive erythropoiesis produced by overexpression of Epo (comparable to the effect of our Epo-inj mouse model of secondary polycythemia) showed degeneration in multiple tissue types, including the brain [57]. In addition, case studies of patients with ET and PV report neurological symptoms such as depression [9], mixed movement disorder [10], amnesia, headache and dysphagia. In a retrospective study, PV patients with an elevated hematocrit that

presented with transient blindness episodes showed reduced blood flow in the retina as compared with controls [58]. After phlebotomy to lower the hematocrit value to a normal range, retinal blood flow improved (but was still below controls) and transient blindness episodes were eliminated in almost all patients. Finally, in a prospective study of ET patients, neurological symptoms including blurry vision, headache, tinnitus and dizziness were reported [12]. Therapies that decrease capillary stalling could play an important role in reducing microvascular thrombotic and vasomotor complications of the MPNs, including not only neurological disorders but also others such as erythromelalgia, which is caused by capillary occlusions in the extremities.

The longstanding uncertainties about the basic mechanisms of microcirculatory dysfunction in the MPNs have led to inadequate attention to potential neurological impacts, despite evidence of neurological disease and of microcirculatory problems in other parts of the body in MPN patients. Our introduction of an *in vivo* animal model that permits direct visualization and measurement of blood flow disruptions in the cortical microvasculature in real time enables identification of the cellular mechanisms underlying microcirculatory dysfunction. We used advanced *in vivo* imaging techniques to directly demonstrate impaired cerebral blood flow in mouse models of PV, ET, mixed MPN and secondary polycythemia for the first time, and found that it is caused not necessarily by problems in larger arterioles or venules, but rather by plugging of individual capillary segments. In ET models, platelet aggregates caused the majority of the capillary stalls, suggesting platelet activation plays a role. In PV models, adhered RBCs caused the majority of the capillary stalls. Our studies provide novel insights into the hemodynamic and cellular mechanisms of cerebral microcirculatory disturbances in ET and PV. This approach could open the door to the rational evaluation of therapeutic targets that may alleviate microvascular complications observed in MPNs.

Addendum

T. P. Santisakultarm, N. Nishimura, W. L. Olbricht, A. I. Schafer, R. T. Silver and C. B. Schaffer designed the research and analyzed the results. T. P. Santisakultarm and C. Q. Paduano performed the experiments and data analysis. T. Stokol and T. L. Southard analyzed blood and bone marrow to phenotype animals. R. C. Skoda designed and provided the transgenic mice. T. P. Santisakultarm and C. B. Schaffer wrote the manuscript. All authors reviewed and commented on the manuscript.

Acknowledgements

We thank G. L. Otte for the development of the algorithm to stitch three-dimensional image stacks.

Sources of funding

This work was supported by a grant from the Judy and William Higgins Trust of the Cancer Research and Treatment Fund, Inc. New York, NY (C. B. Schaffer) and by a Med-into-Grad Fellowship from the Howard Hughes Medical Institute (T. P. Santisakultarm).

Disclosure of Conflict of Interests

The authors state that they have no conflicts of interest.

Supporting Information

Additional Supporting Information may be found in the online version of this article:

Fig. S1. Leukocyte and platelet counts did not predict cortical capillary stall rate.
Fig. S2. Capillary stalls associated with leukocyte plugs, platelet aggregates, stagnant RBCs and empty vessels in MPN mouse models reestablished blood flow at unequal rates.
Fig. S3. Capillary density in ET, PV, mixed MPN and secondary erythrocytosis mouse models.
Table S1. Number of subjects in each measurement.
Video S1. 2PEF image stack from a BMT PV mouse.

References

1 Tefferi A. The history of myeloproliferative disorders: before and after Dameshek. *Leukemia* 2008; **22**: 3–13.
2 Spivak JL, Barosi G, Tognoni G, Barbui T, Finazzi G, Marchioli R, Marchetti M. Chronic myeloproliferative disorders. *Hematology Am Soc Hematol Educ Program* 2003; **2003**: 200–24.
3 Wood JH, Kee DB Jr. Hemorheology of the cerebral circulation in stroke. *Stroke* 1985; **16**: 765–72.
4 Kurabayashi H, Hishinuma A, Uchida R, Makita S, Majima M. Delayed manifestation and slow progression of cerebral infarction caused by polycythemia rubra vera. *Am J Med Sci* 2007; **333**: 317–20.
5 Segura T, Serena J, Teruel J, Davalos A. Cerebral embolism in a patient with polycythemia rubra vera. *Eur J Neurol* 2000; **7**: 87–90.
6 Vermeer SE, Prins ND, den Heijer T, Hofman A, Koudstaal PJ, Breteler MM. Silent brain infarcts and the risk of dementia and cognitive decline. *N Engl J Med* 2003; **348**: 1215–22.
7 Erkinjuntti T, Haltia M, Palo J, Sulkava R, Paetau A. Accuracy of the clinical diagnosis of vascular dementia: a prospective clinical and post-mortem neuropathological study. *J Neurol Neurosurg Psychiatry* 1988; **51**: 1037–44.
8 Kovari E, Gold G, Herrmann FR, Canuto A, Hof PR, Bouras C, Giannakopoulos P. Cortical microinfarcts and demyelination affect cognition in cases at high risk for dementia. *Neurology* 2007; **68**: 927–31.
9 Fones C, Tsoi WF. Polycythaemia rubra vera presenting with depression: recognising the syndrome abulia. *Br J Clin Pract* 1995; **49**: 97–9.
10 Bauer M. Absolutely therapy-resistant depression and mixed movement disorder in an unusual case of polycythemia vera. *Pharmacopsychiatry* 1995; **28**: 66–8.

11 Richard S, Perrin J, Baillot PA, Lacour JC, Ducrocq X. Ischaemic stroke and essential thrombocythemia: a series of 14 cases. *Eur J Neurol* 2011; **18**: 995–8.

12 Billot S, Kouroupi EG, Le Guilloux J, Cassinat B, Jardin C, Laperche T, Fenaux P, Carpentier AF, Kiladjian JJ. Neurological disorders in essential thrombocythemia. *Haematologica* 2011; **96**: 1866–9.

13 Levine RL, Wadleigh M, Cools J, Ebert BL, Wernig G, Huntly BJ, Boggon TJ, Wlodarska I, Clark JJ, Moore S, Adelsperger J, Koo S, Lee JC, Gabriel S, Mercher T, D'Andrea A, Frohling S, Dohner K, Marynen P, Vandenberghe P, *et al*. Activating mutation in the tyrosine kinase JAK2 in polycythemia vera, essential thrombocythemia, and myeloid metaplasia with myelofibrosis. *Cancer Cell* 2005; **7**: 387–97.

14 James C, Ugo V, Le Couedic JP, Staerk J, Delhommeau F, Lacout C, Garcon L, Raslova H, Berger R, Bennaceur-Griscelli A, Villeval JL, Constantinescu SN, Casadevall N, Vainchenker W. A unique clonal JAK2 mutation leading to constitutive signalling causes polycythaemia vera. *Nature* 2005; **434**: 1144–8.

15 Baxter EJ, Scott LM, Campbell PJ, East C, Fourouclas N, Swanton S, Vassiliou GS, Bench AJ, Boyd EM, Curtin N, Scott MA, Erber WN, Green AR, Cancer Genome Project. Acquired mutation of the tyrosine kinase JAK2 in human myeloproliferative disorders. *Lancet* 2005; **365**: 1054–61.

16 Morgan KJ, Gilliland DG. A role for JAK2 mutations in myeloproliferative diseases. *Annu Rev Med* 2008; **59**: 213–22.

17 Tiedt R, Hao-Shen H, Sobas MA, Looser R, Dirnhofer S, Schwaller J, Skoda R. Ratio of mutant JAK2-V617F to wild-type Jak2 determines the MPD phenotypes in transgenic mice. *Blood* 2008; **111**: 3931–40.

18 Santisakultarm TP, Schaffer CB. Optically quantified cerebral blood flow. *J Cereb Blood Flow Metab* 2011; **31**: 1337–8.

19 Kleinfeld D, Mitra PP, Helmchen F, Denk W. Fluctuations and stimulus-induced changes in blood flow observed in individual capillaries in layers 2 through 4 of rat neocortex. *Proc Natl Acad Sci U S A* 1998; **95**: 15741–6.

20 Kubovcakova L, Lundberg P, Grisouard J, Hao-Shen H, Romanet V, Andraos R, Murakami M, Dirnhofer S, Wagner KU, Radimerski T, Skoda RC. Differential effects of hydroxyurea and INC424 on mutant allele burden and myeloproliferative phenotype in a JAK2-V617F polycythemia vera mouse model. *Blood* 2013; **121**: 1188–99.

21 Santisakultarm TP, Cornelius NR, Nishimura N, Schafer AI, Silver RT, Doerschuk PC, Olbricht WL, Schaffer CB. *In vivo* two-photon excited fluorescence microscopy reveals cardiac- and respiration-dependent pulsatile blood flow in cortical blood vessels in mice. *Am J Physiol Heart Circ Physiol* 2012; **302**: H1367–77.

22 Baatz H, Steinbauer M, Harris AG, Krombach F. Kinetics of white blood cell staining by intravascular administration of rhodamine 6G. *Int J Microcirc Clin Exp* 1995; **15**: 85–91.

23 Nguyen QT, Tsai PS, Kleinfeld D. MPScope: a versatile software suite for multiphoton microscopy. *J Neurosci Methods* 2006; **156**: 351–9.

24 Pologruto TA, Sabatini BL, Svoboda K. ScanImage: flexible software for operating laser scanning microscopes. *Biomed Eng Online* 2003; **2**: 13.

25 Schaffer CB, Friedman B, Nishimura N, Schroeder LF, Tsai PS, Ebner FF, Lyden PD, Kleinfeld D. Two-photon imaging of cortical surface microvessels reveals a robust redistribution in blood flow after vascular occlusion. *PLoS Biol* 2006; **4**: e22.

26 Reikvam H, Tiu RV. Venous thromboembolism in patients with essential thrombocythemia and polycythemia vera. *Leukemia* 2012; **26**: 563–71.

27 Knottnerus IL, Ten Cate H, Lodder J, Kessels F, van Oostenbrugge RJ. Endothelial dysfunction in lacunar stroke: a systematic review. *Cerebrovasc Dis* 2009; **27**: 519–26.

28 Basquiera AL, Soria NW, Ryser R, Salguero M, Moiraghi B, Sackmann F, Sturich AG, Borello A, Berretta A, Bonafe M, Barral JM, Palazzo ED, Garcia JJ. Clinical significance of V617F mutation of the JAK2 gene in patients with chronic myeloproliferative disorders. *Hematology* 2009; **14**: 323–30.

29 Panova-Noeva M, Marchetti M, Spronk HM, Russo L, Diani E, Finazzi G, Finazzi G, Salmoiraghi S, Rambaldi A, Barbui T, Ten Cate H, Falanga A. Platelet-induced thrombin generation by the calibrated automated thrombogram assay is increased in patients with essential thrombocythemia and polycythemia vera. *Am J Hematol* 2011; **86**: 337–42.

30 Marchioli R, Finazzi G, Specchia G, Cacciola R, Cavazzina R, Cilloni D, De Stefano V, Elli E, Iurlo A, Latagliata R, Lunghi F, Lunghi M, Marfisi RM, Musto P, Masciulli A, Musolino C, Cascavilla N, Quarta G, Randi ML, Rapezzi D, *et al*. Cardiovascular events and intensity of treatment in polycythemia vera. *N Engl J Med* 2013; **368**: 22–33.

31 Wautier MP, El Nemer W, Gane P, Rain JD, Cartron JP, Colin Y, le van Kim C, Wautier JL. Increased adhesion to endothelial cells of erythrocytes from patients with polycythemia vera is mediated by laminin alpha5 chain and Lu/BCAM. *Blood* 2007; **110**: 894–901.

32 Wautier JL, Wautier MP. Molecular basis of erythrocyte adhesion to endothelial cells in diseases. *Clin Hemorheol Microcirc* 2013; **53**: 11–21.

33 Rahuel C, Filipe A, Ritie L, El Nemer W, Patey-Mariaud N, Eladari D, Cartron JP, Simon-Assmann P, le van Kim C, Colin Y. Genetic inactivation of the laminin alpha5 chain receptor Lu/BCAM leads to kidney and intestinal abnormalities in the mouse. *Am J Physiol Renal Physiol* 2008; **294**: F393–406.

34 Wandersee NJ, Olson SC, Holzhauer SL, Hoffmann RG, Barker JE, Hillery CA. Increased erythrocyte adhesion in mice and humans with hereditary spherocytosis and hereditary elliptocytosis. *Blood* 2004; **103**: 710–6.

35 Spivak J. Daily aspirin–only half the answer. *N Engl J Med* 2004; **350**: 99–101.

36 Kwaan HC, Wang J. Hyperviscosity in polycythemia vera and other red cell abnormalities. *Semin Thromb Hemost* 2003; **29**: 451–8.

37 Carobbio A, Thiele J, Passamonti F, Rumi E, Ruggeri M, Rodeghiero F, Randi ML, Bertozzi I, Vannucchi AM, Antonioli E, Gisslinger H, Buxhofer-Ausch V, Finazzi G, Gangat N, Tefferi A, Barbui T. Risk factors for arterial and venous thrombosis in WHO-defined essential thrombocythemia: an international study of 891 patients. *Blood* 2011; **117**: 5857–9.

38 Karakantza M, Giannakoulas NC, Zikos P, Sakellaropoulos G, Kouraklis A, Aktypi A, Metallinos IC, Theodori E, Zoumbos NC, Maniatis A. Markers of endothelial and *in vivo* platelet activation in patients with essential thrombocythemia and polycythemia vera. *Int J Hematol* 2004; **79**: 253–9.

39 Burgaleta C, Gonzalez N, Cesar J. Increased CD11/CD18 expression and altered metabolic activity on polymorphonuclear leukocytes from patients with polycythemia vera and essential thrombocythemia. *Acta Haematol* 2002; **108**: 23–8. 63063.

40 Schmid-Schonbein GW. Biomechanics of microcirculatory blood perfusion. *Annu Rev Biomed Eng* 1999; **1**: 73–102.

41 Gangat N, Strand J, Li C, Wu W, Pardanani A, Tefferi A. Leucocytosis in polycythaemia vera predicts both inferior survival and leukaemic transformation. *Br J Haematol* 2007; **138**: 354–8.

42 Barbui T, Carobbio A, Rambaldi A, Finazzi G. Perspectives on thrombosis in essential thrombocythemia and polycythemia vera: is leukocytosis a causative factor? *Blood* 2009; **114**: 759–63.

43 Tefferi A. Platelet count in essential thrombocythemia: the more the better? *Blood* 2008; **112**: 3526; author reply -7.

44 Wolanskyj AP, Schwager SM, McClure RF, Larson DR, Tefferi A. Essential thrombocythemia beyond the first decade: life

expectancy, long-term complication rates, and prognostic factors. *Mayo Clin Proc* 2006; **81**: 159–66.
45 Carobbio A, Antonioli E, Guglielmelli P, Vannucchi AM, Delaini F, Guerini V, Finazzi G, Rambaldi A, Barbui T. Leukocytosis and risk stratification assessment in essential thrombocythemia. *J Clin Oncol* 2008; **26**: 2732–6.
46 Tefferi A, Gangat N, Wolanskyj A. The interaction between leukocytosis and other risk factors for thrombosis in essential thrombocythemia. *Blood* 2007; **109**: 4105.
47 Arellano-Rodrigo E, Alvarez-Larran A, Reverter JC, Colomer D, Villamor N, Bellosillo B, Cervantes F. Platelet turnover, coagulation factors, and soluble markers of platelet and endothelial activation in essential thrombocythemia: relationship with thrombosis occurrence and JAK2 V617F allele burden. *Am J Hematol* 2009; **84**: 102–8.
48 Belotti A, Elli E, Speranza T, Lanzi E, Pioltelli P, Pogliani E. Circulating endothelial cells and endothelial activation in essential thrombocythemia: results from CD146+ immunomagnetic enrichment–flow cytometry and soluble E-selectin detection. *Am J Hematol* 2012; **87**: 319–20.
49 Duchemin J, Ugo V, Ianotto JC, Lecucq L, Mercier B, Abgrall JF. Increased circulating procoagulant activity and thrombin generation in patients with myeloproliferative neoplasms. *Thromb Res* 2010; **126**: 238–42.
50 Falanga A, Marchetti M, Evangelista V, Vignoli A, Licini M, Balicco M, Manarini S, Finazzi G, Cerletti C, Barbui T. Polymorphonuclear leukocyte activation and hemostasis in patients with essential thrombocythemia and polycythemia vera. *Blood* 2000; **96**: 4261–6.
51 Arellano-Rodrigo E, Alvarez-Larran A, Reverter JC, Villamor N, Colomer D, Cervantes F. Increased platelet and leukocyte activation as contributing mechanisms for thrombosis in essential thrombocythemia and correlation with the JAK2 mutational status. *Haematologica* 2006; **91**: 169–75.
52 Falanga A, Marchetti M, Vignoli A, Balducci D, Barbui T. Leukocyte-platelet interaction in patients with essential thrombocythemia and polycythemia vera. *Exp Hematol* 2005; **33**: 523–30.
53 Schafer AI. Molecular basis of the diagnosis and treatment of polycythemia vera and essential thrombocythemia. *Blood* 2006; **107**: 4214–22.
54 Zangari M, Fink L, Tolomelli G, Lee JC, Stein BL, Hickman K, Swierczek S, Kelley TW, Berno T, Moliterno AR, Spivak JL, Gordeuk VR, Prchal JT. Could hypoxia increase the prevalence of thrombotic complications in polycythemia vera? *Blood Coagul Fibrinolysis* 2013; **24**: 311–6.
55 O'Brien JT. Vascular cognitive impairment. *Am J Geriatr Psychiatry* 2006; **14**: 724–33.
56 Schmidt WP, Roesler A, Kretzschmar K, Ladwig KH, Junker R, Berger K. Functional and cognitive consequences of silent stroke discovered using brain magnetic resonance imaging in an elderly population. *J Am Geriatr Soc* 2004; **52**: 1045–50.
57 Heinicke K, Baum O, Ogunshola OO, Vogel J, Stallmach T, Wolfer DP, Keller S, Weber K, Wagner PD, Gassmann M, Djonov V. Excessive erythrocytosis in adult mice overexpressing erythropoietin leads to hepatic, renal, neuronal, and muscular degeneration. *Am J Physiol Regul Integr Comp Physiol* 2006; **291**: R947–56.
58 Yang HS, Joe SG, Kim JG, Park SH, Ko HS. Delayed choroidal and retinal blood flow in polycythaemia vera patients with transient ocular blindness: a preliminary study with fluorescein angiography. *Br J Haematol* 2013; **161**: 745–7.